Alpha 9 integrin expression enables reconstruction of the spinal cord sensory pathway.

Katerina Stepankova[1,2], Barbora Smejkalova[1,2], Lucia Machova-Urdzikova[1], Katerina Haveliková[1,2,] Joost Verhaagen[3], Fred de Winter[3], Vit Herynek[4], Jessica Kwok[1,5], James Fawcett[1,6], Pavla Jendelova[1,2]

[1]*Institute of Experimental Medicine Czech Academy of Science, Videnska 1083, 14220 Prague, Czech Republic*

[2]*2nd Faculty of Medicine, Charles University, V uvalu 84, 15006 Prague, Czech Republic*

[3]*Laboratory for Regeneration of Sensorimotor Systems, The Netherlands Institute for Neuroscience, Royal Netherlands Academy of Arts and Sciences (KNAW), Meibergdreef 47, Amsterdam 1105BA, The Netherlands.*

[4]*Center for Advanced Preclinical Imaging, First Faculty of Medicine, Charles University, Salmovská 3, 120 00, Prague 2, Czech Republic*

[5]*Faculty of Biological Sciences, University of Leeds, UK*

[6]*John van Geest Centre for Brain Repair, Department of Clinical Neurosciences, University of Cambridge, CB2 0PY, UK*

Corresponding address:

Institute of Experimental Medicine, CAS

Videnska 1083

142 00 Prague 4

Czechia

Phone no: +420241062828

pavla.jendelova@iem.cas.cz

Running title: Activated integrin and sensory regeneration

Key words: Spinal cord injury, axon regeneration, integrins, kindlin, AAV vectors, sensory testing, cFos,

Abstract

Sensory axons cut within the spinal cord do not regenerate spontaneously. This failure is due in part to absence of an appropriate adhesion molecule on sensory axons, able to interact with the CNS environment. Previous work has shown that transduction of sensory neurons with α9 integrin, which combines with endogenous β1 as α9β1 together with the integrin activator kindlin-1 enables regeneration of sensory axons from a dorsal root crush to the brainstem. The integrin provides an adhesion molecule that recognizes Tenascin-C (which is upregulated in damaged spinal cord) and signals

to upregulate the regeneration-associated gene programme. Regeneration from sensory neurons transduced with α9 integrin and kindlin-1 was examined after C4 and after T10 dorsal column lesions with C6,7 and L4,5 sensory ganglia injected with AAV1 vectors. In α9 integrin and kindlin-1 treated animals sensory axons regenerated through tenascin-C-expressing connective tissue strands and bridges across the lesion then re-entered CNS tissue. Many axons regenerated rostrally to the level of the medulla but were excluded from the sensory nuclei. Regenerated axons were seen particularly at the white matter/grey matter boundary in the dorsal cord. Many branches into the dorsal horn were seen tipped with synaptic swellings. Stimulation of the sciatic nerve led to many neurons rostral to the injury being activated to express cFos. Behavioural recovery was seen in heat and pressure sensation and tape removal. Treatment of sensory neurons with α9 integrin and kindlin-1 therefore enables partial reconstruction of the spinal sensory pathway.

Significance Statement

Full recovery from spinal cord injury can only occur if the axon pathways that connect the brain and spinal cord regenerate to restore motor and sensory connections. Neither sensory nor motor axons in mammals can regenerate spontaneously. A critical factor missing in adult neurons is an adhesion molecule that can enable them to interact with the environment of the damaged spinal cord. In this study in rats an integrin adhesion molecule together with its activator was expressed in sensory neurons using a viral vector. Possession of this adhesion molecule enabled sensory axons to regenerate through the spinal cord injury and all the way back to the brainstem, restoring the sensory pathway. The animal regained touch sensation, enabling sensory behaviours.

Introduction

Sensory neurons in dorsal root ganglia (DRGs) send connections via peripheral nerves (PNS) and through the dorsal root into the spinal cord. When peripheral nerves are crushed many of the sensory axons regenerate back to skin and muscles, while damaged central branch axons show only a small regenerative response. After peripheral axotomy, DRG neurons express a genetic programme including many regeneration-associated genes (RAGs)(Chandran et al., 2016; Ma and Willis, 2015; Tetzlaff et al., 1991) and the Schwann cells transform to a regeneration-permissive state (Arthur-Farraj et al., 2012). In this permissive state the Schwann cell surface contains axon growth-promoting extracellular matrix (ECM) molecules and various growth-promoting trophic factors are secreted. After sensory axons are damaged following spinal cord injury these events do not occur: the RAGs programme is not upregulated, and the glia in the cord and around the injury do not provide an environment that is permissive to axon growth. In particular, the parenchyma of the damaged cord does not provide ECM ligands that are recognized by sensory neuron integrins (Fernandes et al., 1999; Forbes and Andrews, 2017; Mahar and Cavalli, 2018). Cell migration events such as axon regeneration are dependent on a ligand in the environment matched to a receptor in the cell (Caswell and Norman, 2006). In a previous study DRG neurons were transduced with an integrin matched to the CNS environment. α9 integrin is a migration-inducing receptor for tenascin-C, an ECM integrin ligand which is present throughout the CNS ECM and upregulated around injuries (Camand et al., 2004; Tang et al., 2003). Additionally, the integrin activator kindlin-1 was co-transduced into the neurons to prevent inactivation of the integrins by inhibitory chondroitin sulphate proteoglycans (CSPGs) and NogoA (Tan et al., 2012). When these transduced neurons were axotomized in the dorsal root, sensory axons were able to regenerate back into the spinal cord and through the cord up to the level of the medulla (Cheah et al., 2016). A subsequent study to profile mRNA changes in these transduced and regenerating neurons revealed that transduction with α9 integrin and kindlin-1 (α9-K1) upregulated the neuronal RAGs programme, and that axotomy and regeneration additionally upregulated a distinctive CNS regeneration programme that included many genes associated with autophagy, ubiquitination, protein degradation and axonal transport (Cheah et al., 2021). Transduction with α9-K1 therefore provides to sensory neurons axotomized in the CNS the mechanisms that enable regeneration after PNS lesions, namely expression of the RAGs programme and an adhesion molecule matched to the environment. In the current study we have transduced sensory neurons with α9-K1 at the same time as performing dorsal spinal cord injuries at either C4 or T10 levels. This study investigates the ability of the transduced axotomized axons to traverse the chaotic environment of the damaged spinal cord, which includes reactive glia, fibroblast-like cells derived from the meninges, blood vessels, pericytes and inflammatory cells. The ability of axons that cross the lesion to regenerate up the spinal cord is then studied. We show that α9-K1-transduced axons regenerate vigorously through the spinal cord injury core, associating with cells that express tenascin-C and are then able to re-enter the CNS environment where they can regenerate as far as the medulla. The regenerated axons send side-branches into the dorsal horn of the spinal cord where they stimulate propriospinal neurons, and mediate full recovery of sensory functions.

Materials and methods

Preparation of AAV1 vectors

The plasmids AAV-SYN-α9-V5, and AAV-CMV-kindlin1-GFP were amplified and sequenced before proceeding to be packaged into AAV1 as described previously (Hermens et al., 1999). For virus

production, HEK293T cells were transfected with the individual expression and helper plasmids and kept for three days in culture. The transfected cells were then lysed by using 3 freeze-thaw cycles. After centrifugation, the crude lysate was subjected to iodixanol gradient (15%, 25%, 40% and 60%) ultracentrifugation using a Type 70Ti rotor (Beckman) at 490000 x *g*, 16°C for 70 min. The virus was then collected and concentrated using an Amicon Ultra-15 device (Millipore). The titer of the virus was then determined by using real-time quantitative PCR 2.34 x 10^{12} GC/ml for AAV1-α9-V5 and 4.99 x 10^{12} GC/ml for AAV1-kindlin1-GFP. AAV1-SYN-GFP was purchased from Vigene (distributed by Charles River) and the titer was diluted from 2.0 x 10^{13} GC/ml to 2.0 x 10^{12} GC/ml.

Experimental animals and animal surgeries

The present study involved 72 female Lister-Hooded rats (150-175 g; Envigo). Rats were housed by three in cages with a 12-hour light/dark cycle with standard conditions: temperature (22 ± 2°C) and humidity (50% ± 5%). Rats had free access to tapped water and food *ad libitum*.

All procedures were approved by the ethical committee of the Institute of Experimental medicine of ASCR and performed in accordance with Law No. 77/2004 of the Czech Republic. Based on previous studies, the number of animals had been statistically optimized for each particular experiment to achieve their reduction according to European Commission Directive 2010/63/EU, and all efforts were made to minimize pain and suffering. Each animal was allocated a number and randomly assigned to one of the control or experimental groups. The experimenter was blinded throughout the entire study, including behavioural testing and axon quantification.

In order to compare the forelimb and hindlimb sensory regeneration after viral vector administration, the animals were randomly divided into 2 cohorts (n=36 per cohort). One cohort underwent the C4 level of injury with C6 and C7 DRG injections (for forelimb sensory functions restoration). The second cohort underwent the T10 lesion with L4 and L5 DRG injections (for hindlimb sensory functions restoration).

Surgical procedures were performed under an inhalational anaesthetic isoflurane (1.8-2.2%; Baxter Healthcare Pty Ltd; #26675-46-7) in 0.3 l/min oxygen and 0,6 l/min air. All animals received buprenorphine (Vetergesic® Multidose) subcutaneously at a dose of 0.2 mg/kg body weight. Using sterilized surgical equipment, two DRGs (C6, C7 or L4, L5 depending on the cohort) on the left side were exposed and 1 μl of viral vector at a working titre of 2x10^{12} GC/ml was manually injected using Hamilton syringe with custom-made needles (Hamilton; specification: 33 gauge, 12mm, PST3). At the same time, a concurrent laminectomy at the C4 or T10 level (depending on the cohort) was performed. A small slit was pierced in the dura with Insulin syringe U100 (B Braun Omnican 50 Insulin Syringes; #9151117S), and the dorsal columns were crushed with a pair of fine Bonn forceps (Fine Science Tools). The tips of the Bonn forceps were held on either side of the dorsal columns where the small slits were made, pushed 1 mm down into the spinal cord, and then held tightly together for 15s. This lesion has been shown in many previous studies to cause a complete transection of the dorsal columns down to the level of the spinal canal. Immediately after the injury, muscles and skin were sutured. At the end of the experiment, the animals were intraperitoneally anesthetized with a lethal dose of ketamine (100 mg/kg) and xylazine (20 mg/kg) and perfused intracardially with 4% paraformaldehyde (PFA) in 1X-PBS. Two animals (each from one cohort) died the night after the surgery. We had to humanely euthanize two animals from the thoracic injury cohort for welfare reasons in this study.

Sensory behavioural testing

The mechanical pressure (von Frey test) test, the thermal pain (Hargreaves test) test, and the tape removal test were performed every other week for 12 weeks to ensure that animals did not learn the task independently of sensory reflexes. Animals were placed in the testing room at least 30 minutes before the test to allow adaption. Each rat was measured 3 times before the surgical procedure to obtain a baseline for each test.

Mechanical pressure test

The touch sensitivity was measured with the electronic von Frey test (IITC Inc., Life Science Instruments, Woodland Hills, CA, USA). Animals were placed in the plexiglass enclosure on a mesh floor stand (IITC Inc., Life Science Instruments, Woodland Hills, CA, USA) at least 30 minutes before the test to allow adaption. Paws were then stimulated by a slowly-raising probe with rigid plastic tip to touch the centre of the paw. Pressure was increased until the nociceptive response in the form of paw withdrawal. The value was then recorded. Each paw was measured 5 times, forelimb (cervical SCI cohort) / hindlimb (thoracic SCI cohort), left (experimental) and right (internal control). The lowest and the highest of these five values were deleted and the three remaining values were averaged.

Thermal test

SCI-mediated changes in thermal sensation were measured by the Ugo Basile Plantar Heat test apparatus (Comerio VA, Italy). Rats were placed into a plexiglass box with fiberglass bottom and let habituated there for 30 minutes. An infrared emitting device (Ugo Basile) was then placed directly under the footpad of the forelimb/hindlimb. The time when the rat withdrew its paw was recorded. The heat stimulus and timer were automatically activated simultaneously. The infrared stimulus turned off automatically after 30 s to prevent any harm to the animal. Five trials were performed on each forelimb (cervical SCI cohort) / hindlimb (thoracic SCI cohort), left (experimental) and right (internal control) with at least 3 min pause between individual trials. The average withdrawal time was calculated by averaging the three trials after deleting the lowest and the highest value for each animal.

Tape removal test

For the tape removal test, each rat was trained over 5 sessions and then tested every other week post-surgery. The rat was then released from its home cage, placed in an empty test cage and habituated there for 15 minutes. A small piece of tape (approximately 1 square centimetre) was taped to the paw. Three trials were performed on each forelimb (cervical SCI cohort) / hindlimb (thoracic SCI cohort), left (experimental) and right (internal control) with at least 3 min pause between each trial. Left and right paws were tested simultaneously. The time when the animal first noticed the tape and the time when animal removed the tape was recorded. If the rat did not notice/remove the tape by 5 minutes the tape was removed and a time of 5 min was recorded. For this test the paper tape (TimeMed Labeling Systems, Inc.; Fisher Scientific; #NC9972972) was used.

Electrostimulation

Three animals from each group were terminally anesthetized with urethane (Sigma Aldrich; #U2500) at a dose of 1.5 g/kg. Then median nerve (cervical SCI cohort) or sciatic nerve (thoracic SCI cohort) was exposed. The stimulating electrode was inserted into the nerve and the ground electrode into the nearby

muscle. The stimulation consisted of 10 stimulus trains, with stimulus duration of 0.5 ms with amplitude of 7.2 mA, a frequency of 100 Hz, and train duration of 2 s and 8 s intervals between trains as previously described by Bojovic et al (Bojovic et al., 2016). Used electrodes were single subdermal needles (Rhythmlink) Animals were perfused 2 hours after electrical stimulation.

MRI

After transcardial perfusion, 2 cm long injured spinal cord samples were collected, post-fixed in 4% PFA in PBS (over 2 nights), then transferred to PBS with 0.002% azide in a small plastic tube (1.5 ml) with the cap. Spinal cords were then post mortem visualized using 7T MRI preclinical scanner (MRS*DRYMAG 7.0T, MR Solutions, GB). MRI was done in collaboration with the Center for Advanced Preclinical Imaging (CAPI) in Prague.

Immunostaining

PFA-fixed tissue samples were cryopreserved in sucrose solution with gradually increasing concentration (10%, 20%, and 30% sucrose in deionized water). Samples were transferred from a less concentrated solution to a more concentrated solution after immersion. Tissue was then embedded in OCT mounting media (VWR, #03820168). Sections were cut on slides at 8 μm (DRGs) and at 20 μm (spinal cords) on a cryostat (Thermo Scientific, Cryostar NX70). Sections were permeabilized in 0.5% Triton X-100 (Sigma, #T8787) for 2 h at room temperature (RT) and then blocked in 0.2% Triton X-100 and 10% ChemiBLOCKER (Millipore, #2170) for another 2 h at RT. After blocking, sections were incubated with following primary antibodies and/or labelling agents: anti-GFP (Invitrogen, #11122, 1:800, 3 days or Invitrogen, #10262, 1:800, 3 days), anti-V5 (Invitrogen, #R96025, 1:800, 3 days), anti-cFOS (Abcam, #ab208942, 1:500, 2 days), anti-neurofilament (NF200) (Sigma, #N4142, 1:800, 3 days), anti-IBA4 (Sigma, #L2140, 1:800, 3 days), anti-CGRP (Sigma, #PC205L, 1:800, 3 days), anti-β-III tubulin (Cell Signaling, #5568S, 1:1000, 3 days), anti-laminin (Abcam, #ab11575, 1:800, 3 days), anti-tenascin-C (obtained from Faissner lab, Bochum, Germany, 1:500, days), anti-GFAP-Cy3 (Sigma-Aldrich, #C9205, 1:800, 3 days), and anti-VGLUT1/2 (Synaptic Systems, #1235503, 1:800, 3 days). As secondary antibodies goat anti- host antibodies of the respective primary antibodies conjugated with Alexa Fluor 405, 488, 594 and, 647, (1:300; 4 h, RT, Invitrogen) were used. Tissues were then washed with 0.2% Triton X-100 in PBS and subsequently mounted with Mowiol mounting medium (Carl Roth, #0713.2) with added DABCO to reduce fluorescent signal fading (Carl Roth, #0718.1).

Tissue Clearing for light sheet microscopy

Four randomly chosen DRGs from each group were dehydrated by using ethanol (EtOH) dilution series (30%, 50%, 70%, 100%) with 2% Tween20 (Sigma-Aldrich, #P1379) and then delipidated in DCM with EtOH (2:1). Samples were then rehydrated by serial EtOH diluted solutions (70%, 50%, 30%) with 2% Tween20. Samples were then permeabilized by solution containing 0.2% triton v PBS, 0.3M glycine, 10% DMSO. Samples were blocked in 0.2% triton v PBS, 0.3M glycine, 10% DMSO, and 10% ChemiBLOCKER (2 days, 37°C). After blocking, DRG samples were incubated in the blocking solution with added primary

antibodies: anti-GFP (Invitrogen, #11122, 1:400, 2 days, 37°C), and anti-V5 (Invitrogen, #R96025, 1:400, 2 days, 37°C). Secondary antibodies (1:300) were prepared in blocking solution and applied for 3 days at 37°C. Samples were then dehydrated again by using the same EtOH dilution series as at the beginning, and then cleared in Ethyl Cinnamate (Sigma-Aldrich, #112372) for 2 hours at RT. After clearing and imaging were performed, the DRGs were rehydrated in EtOH diluted solutions (100%, 70%, 50%, 30%), washed in PBS and cryopreserved in sucrose solution (10%, 20%, 30%), sectioned as described previously, and re-used for transduction efficiency analysis.

Microscopy and statistical analysis

Confocal imaging was performed using a Zeiss LSM880 Airyscan microscope and lightsheet imaging was performed using Zeiss Lightsheet Z.1 microscope. Images were analysed semiautomatically using NIH ImageJ or by manual approach using microscope eyepiece reticle net grid, when appropriate. Data processing and statistical analysis were performed using GraphPad Prism (GraphPad Software). Lightsheet data were processed by Huygens Software ((Scientific Volume Imaging, The Netherlands, http://svi.nl) and Imaris Microscopy Image Analysis Software (Oxford Instruments). Data are expressed as mean ±SEM. Statistical differences between groups were determined by one-way or two-way with Tukey's multiple comparisons test. For all statistical analyses, a p value of 0.05 was considered to be significant.

Results

Female adult rats received spinal cord dorsal column lesions at level C4 or T9 and at the same operation received injections of AAVs to DRGs at level C6,7 or L3,4. The three experimental groups received different AAV injections, 1) AAV-GFP (GFP group), 2) AAV-kindlin-1-GFP (kindlin group), 3) AAV-kindlin-1-GFP + AAV-α9 –V5 (α9-kindlin group). AAV-GFP (provides a control for AAV injection, AAV-kindlin-1-GFP shows the effect of activating the integrins that are endogenously expressed in DRG neurons, AAV-kindlin-1-GFP + AAV- α9 –V5 is the regeneration-inducing treatment with the tenascin-binding integrin and its activator. Animals received sensory behavioural testing for 12 weeks, then at week 13 animals were killed for histology. Before this some animals received electrical stimulation to their sciatic or median nerve (Figure 1)

AAVs transduce integrin and kindlin into DRG neurons

Transduction of DRG neurons was assessed by immunostaining of the DRGs and axons below the level of the lesions (Figure 2a). Transduction efficiencies were obtained by counting the ratio of GFP and/or V5-positive cell bodies with βIII-tubulin-positive cell bodies. The transduction efficiency is shown in Table 1. The transduction efficiency was similar for the three vectors. The kindlin1 vector was injected at a 1:3 ratio to compensate for the larger length of the integrin gene.

VIRAL VECTORS	C6, C7 DRGs (%)	L4, L5 DRGs (%)
AAV1-GFP	33.39 ± 1.714	36.59 ± 2.838

AAV1-kindlin-1-GFP	28.98 ± 0.780	39.06 ± 2.973
AAV1-α9-V5	37.24 ± 2.194	32.94 ± 1.575
% βIII tubulin +ve neurons co-transduced with AAV1-α9-V5 + AAV1-kindlin-1-GFP (injected in 3:1 ratio)	21.75 ± 1.392	23.37 ± 1.589
% alpha 9 neurons also +ve for kindlin	62.24 ± 4.570	68.48 ± 2.537

Table 1. Transduction efficiencies of sensory neurons after direct DRG injection. Data are expressed as mean ± SEM, n= 20-24 per group.

To confirm that transduced sensory neurons are located throughout the DRG and not just locally, we imaged transduced DRGs using 3D light-sheet microscopy 13 weeks after AAVs injections. In addition, immunostaining showed that AAV1-α9-V5 and AAV1–kindlin-1–GFP transduced all three sensory neuronal types located in DRGs: large diameter mechanoreceptors (NF200-positive), medium diameter nociceptors (IBA4-positive), and small diameter thermoreceptors (CGRP-positive) (Figure 2b).

The transport of α9-V5 and kindlin-1-GFP in sensory axons caudal to the lesion was visualized by immunostaining. The spinal cord was sectioned at 40µm then every fifth section was stained for V5 and GFP. These molecules transported from the DRGs were used as axon tracers for all the experiments in this study.

The number of axons was counted using an eyepiece grid, counting the number of axons crossing a line of the grid at regular distances caudal and rostral to the lesion. The sum of the values from each distance point was then multiplied by 5 to estimate the number of labelled axons at this level in each spinal cord.

In the dorsal roots as well as in the spinal cord caudal to the lesion, many axons were positive for both α9-V5 and kindlin-1-GFP, but there were also axons that were only positive for one molecule (Figure 2c). The observed average number of labelled axons in the spinal cord below thoracic lesions was:

	Cervical SCI cohort	Thoracic SCI cohort
Kindlin-1-GFP axons	1837 ± 39	1890 ± 45
α9-V5 axons	2465 ± 105	2322 ± 109
Co-transduced axons	1422 ± 124	1375 ± 35

Table 2. Number of labelled axons per spinal cord 600µm caudal to the lesion. Data are expressed as mean ± SEM, n= 3 per group.

Alpha9K1 axons regenerate across lesions in connective tissue bridges

Axons from the integrin 9 + kindlin-1 group were observed to cross the lesion, re-enter CNS tissue and continue to grow rostrally up the cord. Within the lesions many axons were seen in GFAP-negative connective tissue strands and bridges and in the meningeal/connective tissue roof that covered most lesions, with a few regenerating axons growing around the lesion base particularly in cervical lesions (Figure 3a,b). Where the connective tissue interfaced with the rostral lesion margin axons often showed tangles of axons with changes in course (Figure 3c), but once established in CNS tissue, axons followed a fairly straight course. Some axons did not re-enter CNS tissue but were seen growing alongside the cord in the meninges (Figure 3d). In the α9-kindlin we measured 849 ± 64 axons 1mm rostral to the lesion margin.

In GFP controls no axons grew across the lesion, although a few sprouts were seen around the lesion edge and in the caudal margin of the lesion core (Figure 4a). In animals expressing kindlin-1 alone some sensory axon regeneration was seen in the laminin+ve connective tissue within and bridging the lesion, closely in contact with laminin+ve structures, but axons did not re-enter CNS tissue to grow beyond the lesion area (Figure 4b). On the margin of the rostral part of the lesion, the integrin α9-kindlin-1 group showed significantly more axons (819.00 ± 94) to the kindlin-1-only (413± 87; $p = 0.0012$, 2way-ANOVA, n = 10 – 12). However, no axons from kindlin-1-only group continued to grow rostrally above lesion and 1mm above lesion there were no axons visible neither from kindlin-1-only nor from GFP controls.

Alpha9K1 axons regenerate to the brain stem

Animals injected with both, integrin α9 integrin and kindlin-1 (α9-kindlin group), showed regenerating axons rostral to the lesion after both, C4 and T10 injury. Many of these were seen all the way up to the medulla. Most axons were seen at the interface between grey and white matter at the medial edge of the dorsal horns, and a lesser number of axons was seen following a wandering course within the dorsal horn white matter (Figure 5a,b). These regenerating axons were therefore following a different pathway to that of unlesioned sensory axons. Along this regenerated pathway, there were frequent branches extending into the dorsal horn grey matter terminating in arborizations. The distance over which axons regenerated from thoracic lesions reached up to 5cm after thoracic SCI. Almost all the regenerated axons rostral to the lesion stained for both α9-V5 and kindlin-1-GFP (Figure 5c), in contrast to the axons caudal to the lesion, where there was a significant proportion of single-stained axons (Figure 2c). The implication is that only axons containing both α9 and kindlin-1 were able to regenerate through the lesion. Table 2 shows the number of axons regenerating through T10 lesion up to cervical part of spinal cord. Axon regenerative behaviour was similar in both cervical and thoracic lesions.

As in previous studies (Cheah et al., 2016; Massey et al., 2008) no α9-V5 or kindlin-1 +ve axons were seen innervating the two dorsal column sensory nuclei. Axons were seen around the margins of the nuclei but did not enter them (Figure 5d). The absence of labelled axons in the nuclei confirms that the spinal cord lesions completely severed the sensory pathway. A summary of axon behaviour in the three experimental groups with axon counts for the α9-V5 or kindlin-1 +ve axons is shown in Figure 6.

	GFP			**kindlin-1**			**integrin α9 + kindlin-1**		
Distance (mm)	**number of axons**	**SEM**	**RI**	**number of axons**	**SEM**	**RI**	**number of axons**	**SEM**	**RI**
- 0.6	1519	135	NA	1258	144		1653	173	NA
bellow lesion	0	0	NA	1049	140		1475	201	NA
above lesion	0	0	0	413	87	0.328	819	94	0.495
+ 0.6	0	0	0	0	0	0	850	62.	0.514

1	0	0	0	0	0	0	849	64	0.514
6	0	0	0	0	0	0	796	45	0.482
10	0	0	0	0	0	0	784	93	0.474
16	0	0	0	0	0	0	647	91	0.391
30	0	0	0	0	0	0	793	99	0.480
36	0	0	0	0	0	0	640	76	0.387
42	0	0	0	0	0	0	413	47	0.250
48	0	0	0	0	0	0	309	60	0.187

Table 3: Number of axons and regeneration index in GFP, kindlin1 and α9-kindlin group. Data are expressed as mean ± SEM, n=10 (animals/group) NA=not available

Alpha9K1 axons regenerate through tenascin-C containing tissue +

To examine the substrate on which α9-kindlin-1 V5- positive axons grew, immunostaining for GFAP, laminin and tenascin-C was performed. The connective tissue strands and roof in lesions were entirely or partly GFAP negative, usually with a clear boundary between CNS and connective tissue which stained for laminin and tenascin-C (Figure 7a). GFP-positive axons from the kindlin-1 group were seen in association with the laminin substrate. Tenascin-C was strongly positive in the connective tissue and meningeal tissues through which axons of the α9-kindlin group regenerated (Figure 7b). However, the boundary with CNS tissue was less clear than in laminin stains, because the CNS tissue surrounding lesions was positive for tenascin-C. Overall, we found that many axons in the α9-kindlin group were present in the tenascin-C and laminin+ve connective tissue bridges and roof, mostly in regions that were GFAP negative.

In summary, within the lesion axons expressing α9-V5 and kindlin-1 appeared to regenerate preferentially through connective tissue structures that were positive for laminin and tenascin-C, and were then able to re-enter and grow within the tenascin-C-expressing CNS tissue. Axons that express kindlin-1 alone will contain activated forms of the integrins endogenously expressed by sensory neurons, (α4,5,6,7) which are laminin and fibronectin rectors, and these axons grew where laminin is present but did not re-enter the laminin -ve CNS tissue.

Completeness of dorsal column crush

To verify the completeness of the lesion in our dorsal column crush model, we used 7T MRI. All dissected spinal cords were imaged as sagittal and transversal sections (Figure 8). The sections were then compared with the rat anatomical atlas to exclude lesions that were too wide, too deep, or too small. However, no animal was excluded from the study based on the MRI results. Staining of the sensory nuclei allowed further demonstration of lesion completeness because regenerating axons are excluded from them while unlesioned axons innervate the nuclei (Cheah et al., 2016; Massey et al., 2008). Thus, if V5- or GFP-positive axons were observed in sensory nuclei, the lesion would be considered as incomplete.

Regenerating axons make a functional synapse above the lesion

To assess functional connectivity over the lesion, spinal cFOS expression was monitored after electrical stimulation of the median and sciatic nerves. cFOS belongs to the immediate early genes and is a well-established marker of transcription induced by neuronal activity.

To quantify the total number of cFOS+ nuclei in the dorsal horns below (C6 or L1 level) and above the lesion (C2 and Th8 level), the Cell Counter plugin in ImageJ (Schindelin et al., 2012) was used. For each animal, three adjacent sections below and above lesion were analysed, and then the mean of each subset was calculated. The results are presented as a percentage of the ratio of the number of cFOS-positive cells above the lesion to the number of cFOS-positive cells below the lesion. A significantly higher percentage of cFOS-positive cells was observed in the integrin α9 – kindlin-1 group (32.656 $\pm$ 3.305 % after cervical SCI and 44.380 $\pm$ 2.684 % after thoracic SCI) compared to the GFP (5. 369 $\pm$ 1.451 % after cervical SCI and 7.754 $\pm$ 1.334 % after thoracic SCI) and kindlin-1 (11.084 $\pm$ 2.759 % after cervical SCI and 9.650 $\pm$ 1.313 % after thoracic SCI) groups (Figure 9a). The differences between α9 – kindlin-1 and GFP groups were significant (P=<0.0001). No significance was observed between the GFP and kindlin-1 groups in either cohort.

Using super resolution, V5-positive sensory axon terminals were observed in spinal coronal section taken above lesion in colocalization with VGluT1/2 puncta, indicating functional synaptic reconnection (Figure 9b). These data show that regenerated axons in the α9 – kindlin-1 group were able to establish functional synapses rostral to the lesions.

alpha9K1 restored sensory functions

To examine sensory behavioural recovery, tests of forelimb and hindlimb function were used for animals with C4 lesions/cervical injections and T10 lesions/lumbar injections respectively. A soft mechanical pressure (Von Frey) test, a heat test (Plantar/Hargreaves) and a tape removal test were used (Figure 10). The tests started 2 weeks before the surgery (pre-test period) to obtain reference values for healthy animals and also to allow the animals to learn the required task. The week after surgery represented a testing break to allow the animals to adapt to the new pathophysiological conditions. From the second week of viral expression, animals were tested every other week for 12 weeks.

During the first testing week, the experimental left paw and the internal control right paw showed a significant sensory deficit after both levels of injury, cervical and thoracic compared to the reference values. Sensory deficits were manifested by greater force required to elicit withdrawal in the mechanical pressure test, longer withdrawal time in the heat test and longer delay time with tape in the tape removal test.

In the mechanical pressure test, the integrin α9- kindlin-1 group began to show significant recovery compared to the GFP group from week 6 in the cervical SCI cohort ($p = 0.0287$, 2way-ANOVA, n =11-12) and from week 8 in the thoracic SCI cohort ($p = 0.0006$, 2way-ANOVA, n =10-12). In the cervical SCI cohort, the kindlin-1 only group also showed significant but lesser recovery compared to the GFP group ($p = 0.0007$, 2way-ANOVA, n =11-12) starting at week 6. The other 2 groups (GFP and kindlin-1 only) in thoracic SCI cohort showed no significant recovery.

In the heat test, both groups, kindlin-1 only and integrin α9 – kindlin-1 showed significant recovery ($p < 0.0001$, 2way-ANOVA, n = 11-12 per group) compared to the GFP group in the cervical SCI cohort. The significant differences started in week 6. After thoracic SCI, only the integrin α9 – kindlin-1 group showed

significant recovery compared to GFP control group ($p = 0.0002$, 2way-ANOVA, n = 10-12 from week 4 but there was no recovery in the other groups.

In the tape removal test, both groups, kindlin-1 only ($p = 0.0162$, 2way-Anova, n = 10-12) and integrin $\alpha 9$ – kindlin-1 ($p = 0.0107$, 2way-Anova, n = 10-12) showed significant recovery compared to the GFP group in cervical SCI cohort. Significant recovery was observed from week 6, however, by week 10 the significant difference disappeared, which we attribute to the animals having learned the task and quickly removing the tape guided by vision instead of sensory perception. After thoracic SCI, significant recovery was only observed in integrin $\alpha 9$ – kindlin-1 group ($p < 0.0001$, 2way-Anova, n = 10-12) compared to the GFP control group. In contrast to the conditions after cervical SCI, the kindlin-1 only group showed no significant recovery after thoracic SCI.

In summary, these results indicate that the integrin $\alpha 9$-kindlin-1 group exhibited superior sensory recovery in both cohorts in the mechanical pressure and heat test. They also performed well in the tape removal test after thoracic SCI. Our results suggest that tape removal test after cervical injury is not ideal for long-term studies such as this, as the animals likely saw the tape on their forepaw before they felt it.

Discussion

This study has demonstrated that α9-K1 transduced neurons regenerated their neurons vigorously through the largely fibroblastic environment of the lesion core of the damaged rat spinal cord. The axons then progressed from this environment back into spinal cord CNS tissue, where they can regenerate up to the level of the medulla, a distance of approx. 4cm from thoracic lesions. Many axonal branches grew into the dorsal horn grey matter, where synapses were evident. On stimulation neurons in the dorsal part of the cord upregulated cFos, indicating that functional connections were formed. Full behavioural recovery was seen for light touch, heat and tape removal.

Mechanisms of axon regeneration

DRG sensory neurons are regeneration-capable, as evidenced by their ability to regenerate axons within the PNS. Extensive regeneration of the axons in the current study suggests that α9-K1 transduction activates mechanisms that allow PNS regeneration, and enable regeneration in the CNS environment. Sensory regeneration in the PNS is associated with upregulation of the RAGs programme of gene expression (Chandran et al., 2016). Several of the molecules expressed in the RAGs programme are necessary for successful regeneration, so regeneration without expression of the RAGs programmed is unlikely. Transduction of sensory neurons with α9-K1, even without axotomy, leads to expression of the RAGs programme, priming the neurons for successful regeneration (Cheah et al., 2021). However, expression of the RAGs programme by itself is not sufficient to enable long-distance spinal sensory regeneration. Crush of peripheral nerves prior to lesion of the central sensory branch upregulates the RAGs programme and leads to increased local sprouting of the cut axons, but not long-distance growth (Neumann and Woolf, 1999). An additional element is therefore required. Cell migration events depend on cell surface growth-promoting receptors that match to ligands in the environment (Caswell and Norman, 2006). This receptor-ligand interaction leads to signalling, increased cytoskeletal dynamics linked to focal adhesions, leading in turn to mechanical traction and migration (Ridley, 2011). The main migration-inducing cell surface adhesion molecules are integrins. Adult DRG neurons express several integrins that bind to fibronectin and laminin (α3β1, α4β1, α5β1 α6β1 and α7β1), with the laminin receptor α7β1 being the main contributor to axon regeneration (Gardiner, 2011; Werner et al., 2000).

However, laminin and fibronectin in the acutely injured cord are found on fibroblastic cells in the lesion core, around blood vessels and on the meninges (Orr and Gensel, 2018; Risling et al., 1993). The integrin ligands in reactive CNS tissue are tenascin-C and osteopontin, which are not partners for the integrins expressed in adult DRGs. The main migration-inducing integrin for tenascin-C and osteopontin is α9β1, and it is therefore not surprising that α9-K1 transduction enables axon regeneration (Hoye et al., 2012). Expression of kindlin-1 alone will activate the integrins endogenously expressed by DRG neurons, which bind to laminin and fibronectin. Therefore kindlin-1 alone allowed sensory axons to regenerate into the lesion core region, but not into CNS tissue for which the axons lack an integrin receptor. Regeneration into the lesion and on into CNS tissue was only seen when neurons were transduced with α9-K1 to provide an activated form of this tenascin-C osteopontin receptor. Unlesioned axons below the lesion in α9-K1 transduced animals mostly expressed both α9 and K1, but some were positive for only one of these. Above the lesion we only saw axons that expressed both α9 and K1, showing that this combination is needed for successful CNS regeneration.

Pathway of axon regeneration

Axons regenerating through the spinal lesion were found associated with strands and bridges of GFAP negative tissue, which has been shown to contain cells of meningeal, vascular, perivascular and fibroblastic origin. These cells expressed laminin and Tenascin-C, and therefore provided a matched growth substrate for endogenously-expressed laminin-binding integrins activated by kindlin-1 and for neurons expressing α9. At the rostral interface between lesion core and CNS tissue, there was usually a region in which axons grew chaotically indicating exploratory behaviour in a disrupted tissue, after which their growth was straight and direct. Within the cord rostral to the lesion regenerating axons in the α9-K1 group were found particularly at the boundary between the dorsal columns and the dorsal horn, with a few axons growing in a wandering fashion through white matter. This differs from the normal pathway of sensory axons, and also differs from the path through white matter that was taken by axons regenerating after α9-K1 and a dorsal root crush (Cheah et al., 2016). We assume that the pathway disruption associated with growth through the lesion cause axons to search for a permissive path, although why the white matter/grey matter boundary should provide this is not obvious. As in previous studies, the regenerating sensory axons did not penetrate the medullary sensory nuclei (Cheah et al., 2016; Massey et al., 2006). This is due to the dense CSPG-rich nets found in these nuclei. We saw less axon regeneration within the cord in animals with cervical lesions and cervical DRG α9-K1 treatment. This was partly due to technical issues, but we also saw more axons in this group continuing to grow beside the spinal cord in meninges rather that re-entering CNS tissue. α9-K1-expressing axons regenerate vigorously in meningeal tissue, and preventing waste of regenerating axons that choose to grow in the meninges rather than spinal cord will be an issue for further development.

Sensory recovery and synapse formation

Many processes were seen growing into the dorsal horns, taking a course perpendicular to the ascending axons. VGLUT1 +ve swellings were seen on these processes, indicating synapse formation. We tested for the ability of these synapses to stimulate neurons in the cord by observing upregulation of cFos in propriospinal neurons after stimulation of the dorsal roots of the α9-K1-injected DRGs. In α9-K1-treated animals the number of cFos neurons after stimulation was much greater than in controls, indicating connections between regenerated axons and cord neurons. This was reflected in sensory recovery tests. Particularly in the lumbar injected α9-K1 group, we saw eventual complete recovery in

fine touch, heat and tape removal tasks. The time course of recovery was similar to the progression of axon regeneration in this and our previous experiment. Recovery in the tape removal task is particularly informative. Animals do not appear to see tape on their hindpaws, unlike the forepaws where tape removal is often triggered by visual recognition. Instead hindpaw tape removal appears to be triggered by sensory recognition. In order to sense that there is tape on the hindpaw, sensation must reach the brain which then executes the removal process. This task therefore shows that regenerating axons carry information to the brain. It is interesting that this occurs in the absence of re-innervation of the medullary sensory nuclei. Presumably sensory information is relayed to the brain from propriospinal neurons that were stimulated by regenerated sensory inputs to the dorsal horn.

The strategy of using an activated integrin to induce sensory regeneration has enabled almost complete reconstruction of the spinal sensory pathway. The regeneration index, comparing axon numbers below and above the lesion indicates that 50% of axons regenerated through the lesion area, and once through the lesion the number of axons did not decline much up to the high cervical cord. However complete reconstruction was not achieved because innervation of the medullary sensory nuclei did not occur. Methods of enabling re-innervation of these nuclei have been identified using chondroitinase digestion and expression of NT3 (Alto et al., 2009; Massey et al., 2006), and these could be applied to bring about a complete tract reconstruction. However, despite lack of innervation of the sensory nuclei functional recovery was almost complete, including tape removal which requires that sensory information must reach the brain. This repair strategy cannot at present be transferred directly to descending motor pathways because in these highly polarized neurons integrins are restricted to the somatodendritic domain and excluded from axons (Andrews et al., 2016; Franssen et al., 2015). Strategies to enable integrin transport to motor axons have been identified, which may make it possible to reconstruct motor pathways (Nieuwenhuis et al., 2020; Petrova et al., 2020).

Acknowledgement:

This work was supported by grants from Czech Ministry of Education, Youth and Sports (CZ.02.1.01/0.0./0.0/15_003/0000419), Medical Research Council (MR/R004463/1, G105497), Wings for Life (WFL GB-04/19), International Foundation for Research in Paraplegia P172, Charles University Grant Agency, project No. 320421 and 102122.

References

Alto, L.T., L.A. Havton, J.M. Conner, E.R. Hollis Ii, A. Blesch, and M.H. Tuszynski. 2009. Chemotropic guidance facilitates axonal regeneration and synapse formation after spinal cord injury. *Nat. Neurosci*. 12:1106-1113.

Andrews, M.R., S. Soleman, M. Cheah, D.A. Tumbarello, M.R.J. Mason, E.B. Moloney, J. Verhaagen, A. Bensadoun, B. Schneider, P. Aebischer, and J.W. Fawcett. 2016. Axonal localization of integrins in the CNS is neuronal type and age dependent. *eneuro*. 3:0029-001Bojovic, O., C.R. Bramham, and A. Tjolsen. 2016. Stimulation-induced expression of immediate early gene proteins in the dorsal horn is increased in neuropathy. *Scand J Pain*. 10:43-51.

Camand, E., M.P. Morel, A. Faissner, C. Sotelo, and I. Dusart. 2004. Long-term changes in the molecular composition of the glial scar and progressive increase of serotoninergic fibre sprouting after hemisection of the mouse spinal cord. *Eur. J. Neurosci*. 20:1161-1176.

Caswell, P.T., and J.C. Norman. 2006. Integrin trafficking and the control of cell migration. *Traffic*. 7:14-21.

Chandran, V., G. Coppola, H. Nawabi, T. Omura, R. Versano, E.A. Huebner, A. Zhang, M. Costigan, A. Yekkirala, L. Barrett, A. Blesch, I. Michaelevski, J. Davis-Turak, F. Gao, P. Langfelder, S. Horvath, Z. He, L. Benowitz, M. Fainzilber, M. Tuszynski, C.J. Woolf, and D.H. Geschwind. 2016. A Systems-Level Analysis of the Peripheral Nerve Intrinsic Axonal Growth Program. *Neuron*. 89:956-970.

Cheah, M., M.R. Andrews, D.J. Chew, E.B. Moloney, J. Verhaagen, R. Fassler, and J.W. Fawcett. 2016. Expression of an Activated Integrin Promotes Long-Distance Sensory Axon Regeneration in the Spinal Cord. *J Neurosci*. 36:7283-7297.

Cheah, M., Y. Cheng, V. Petrova, A. Cimpean, P. Jendelova, V. Swarup, C.J. Woolf, D.H. Geschwind, and J.W. Fawcett. 2021. Integrin-driven Axon Regeneration in the Spinal Cord Activates a Distinctive CNS Regeneration Program. *bioRxiv*:2021.2012.2007.471602.

Fernandes, K.J., D.P. Fan, B.J. Tsui, S.L. Cassar, and W. Tetzlaff. 1999. Influence of the axotomy to cell body distance in rat rubrospinal and spinal motoneurons: differential regulation of GAP-43, tubulins, and neurofilament-M. *J. Comp Neurol*. 414:495-510.

Forbes, L.H., and M.R. Andrews. 2017. Restoring axonal localization and transport of transmembrane receptors to promote repair within the injured CNS: a critical step in CNS regeneration. *Neural Regen Res*. 12:27-30.

Franssen, E.H., R.R. Zhao, H. Koseki, V. Kanamarlapudi, C.C. Hoogenraad, R. Eva, and J.W. Fawcett. 2015. **Exclusion of integrins from CNS axons is regulated by Arf6 activation and the AIS**. *In* J. Neurosci. Vol. in press.

Gardiner, N.J. 2011. Integrins and the extracellular matrix: key mediators of development and regeneration of the sensory nervous system. *Dev Neurobiol*. 71:1054-1072.

Hermens, W.T., O. ter Brake, P.A. Dijkhuizen, M.A. Sonnemans, D. Grimm, J.A. Kleinschmidt, and J. Verhaagen. 1999. Purification of recombinant adeno-associated virus by iodixanol gradient ultracentrifugation allows rapid and reproducible preparation of vector stocks for gene transfer in the nervous system. *Hum Gene Ther*. 10:1885-1891.

Hoye, A.M., J.R. Couchman, U.M. Wewer, K. Fukami, and A. Yoneda. 2012. The newcomer in the integrin family: integrin alpha9 in biology and cancer. *Adv Biol Regul*. 52:326-339.

Ma, T.C., and D.E. Willis. 2015. What makes a RAG regeneration associated? *Front Mol Neurosci*. 8:43.

Mahar, M., and V. Cavalli. 2018. Intrinsic mechanisms of neuronal axon regeneration. *Nat Rev Neurosci*. 19:323-337.

Massey, J.M., J. Amps, M.S. Viapiano, R.T. Matthews, M.R. Wagoner, C.M. Whitaker, W. Alilain, A.L. Yonkof, A. Khalyfa, N.G. Cooper, J. Silver, and S.M. Onifer. 2008. Increased chondroitin sulfate proteoglycan expression in denervated brainstem targets following spinal cord injury creates a barrier to axonal regeneration overcome by chondroitinase ABC and neurotrophin-3. *Exp. Neurol*. 209:426-445.

Massey, J.M., C.H. Hubscher, M.R. Wagoner, J.A. Decker, J. Amps, J. Silver, and S.M. Onifer. 2006. Chondroitinase ABC digestion of the perineuronal net promotes functional collateral sprouting in the cuneate nucleus after cervical spinal cord injury. *J. Neurosci*. 26:4406-4414.

Neumann, S., and C.J. Woolf. 1999. Regeneration of dorsal column fibers into and beyond the lesion site following adult spinal cord injury. *Neuron*. 23:83-91.

Nieuwenhuis, B., A.C. Barber, R.S. Evans, C.S. Pearson, J. Fuchs, A.R. MacQueen, S. van Erp, B. Haenzi, L.A. Hulshof, A. Osborne, R. Conceicao, T.Z. Khatib, S.S. Deshpande, J. Cave, C. Ffrench-Constant, P.D. Smith, K. Okkenhaug, B.J. Eickholt, K.R. Martin, J.W. Fawcett, and R. Eva. 2020. PI 3-kinase

delta enhances axonal PIP3 to support axon regeneration in the adult CNS. *EMBO Mol Med*:e11674.

Orr, M.B., and J.C. Gensel. 2018. Spinal Cord Injury Scarring and Inflammation: Therapies Targeting Glial and Inflammatory Responses. *Neurotherapeutics*. 15:541-553.

Petrova, V., C.S. Pearson, J. Ching, J.R. Tribble, A.G. Solano, Y. Yang, F.M. Love, R.J. Watt, A. Osborne, E. Reid, P.A. Williams, K.R. Martin, H.M. Geller, R. Eva, and J.W. Fawcett. 2020. Protrudin functions from the endoplasmic reticulum to support axon regeneration in the adult CNS. *Nat Commun*. 11:5614.

Ridley, A.J. 2011. Life at the leading edge. *Cell*. 145:1012-1022.

Risling, M., K. Fried, H. Lindå, T. Carlstedt, and S. Cullheim. 1993. Regrowth of motor axons following spinal cord lesions: Distribution of laminin and collagen in the CNS scar tissue. *Brain Res. Bull*. 30:405-414.

Schindelin, J., I. Arganda-Carreras, E. Frise, V. Kaynig, M. Longair, T. Pietzsch, S. Preibisch, C. Rueden, S. Saalfeld, B. Schmid, J.Y. Tinevez, D.J. White, V. Hartenstein, K. Eliceiri, P. Tomancak, and A. Cardona. 2012. Fiji: an open-source platform for biological-image analysis. *Nat Methods*. 9:676-682.

Tan, C.L., M.R. Andrews, J.C. Kwok, T.G. Heintz, L.F. Gumy, R. Fassler, and J.W. Fawcett. 2012. Kindlin-1 enhances axon growth on inhibitory chondroitin sulfate proteoglycans and promotes sensory axon regeneration. *J. Neurosci*. 32:7325-7335.

Tang, X., J.E. Davies, and S.J. Davies. 2003. Changes in distribution, cell associations, and protein expression levels of NG2, neurocan, phosphacan, brevican, versican V2, and tenascin-C during acute to chronic maturation of spinal cord scar tissue. *J Neurosci. Res*. 71:427-444.

Tetzlaff, W., S.W. Alexander, F.D. Miller, and M.A. Bisby. 1991. Response of facial and rubrospinal neurons to axotomy: Changes in mRNA expression for cytoskeletal proteins and GAP-43. *J. Neurosci*. 11:2528-2544.

Werner, A., M. Willem, L.L. Jones, G.W. Kreutzberg, U. Mayer, and G. Raivich. 2000. Impaired axonal regeneration in alpha7 integrin-deficient mice. *J. Neurosci*. 20:1822-1830.

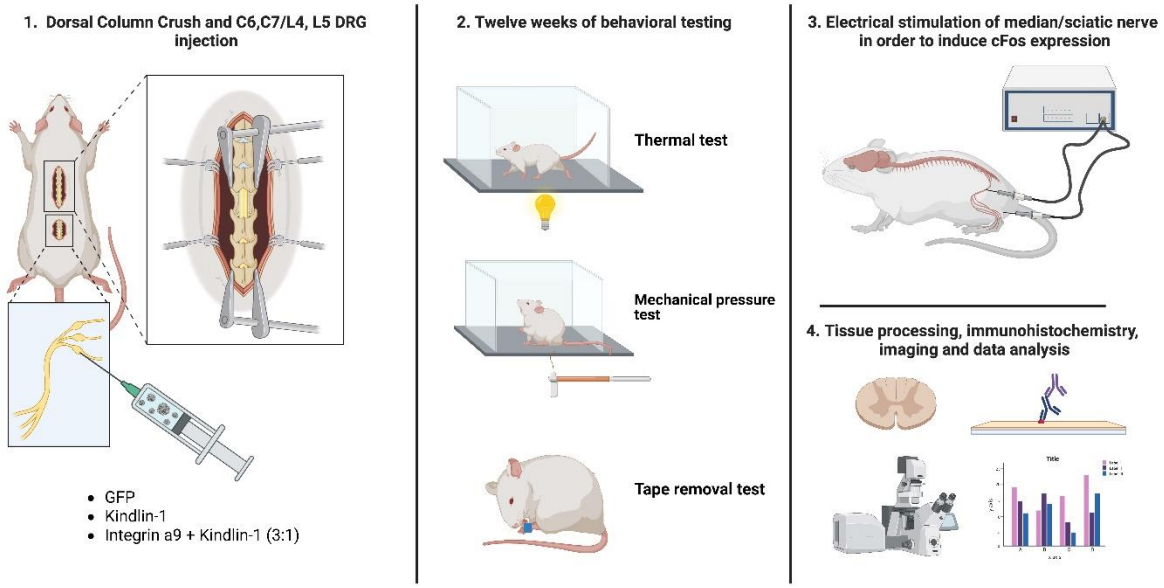

Figure 1

Diagram representing the experimental protocol. Created in Biorender

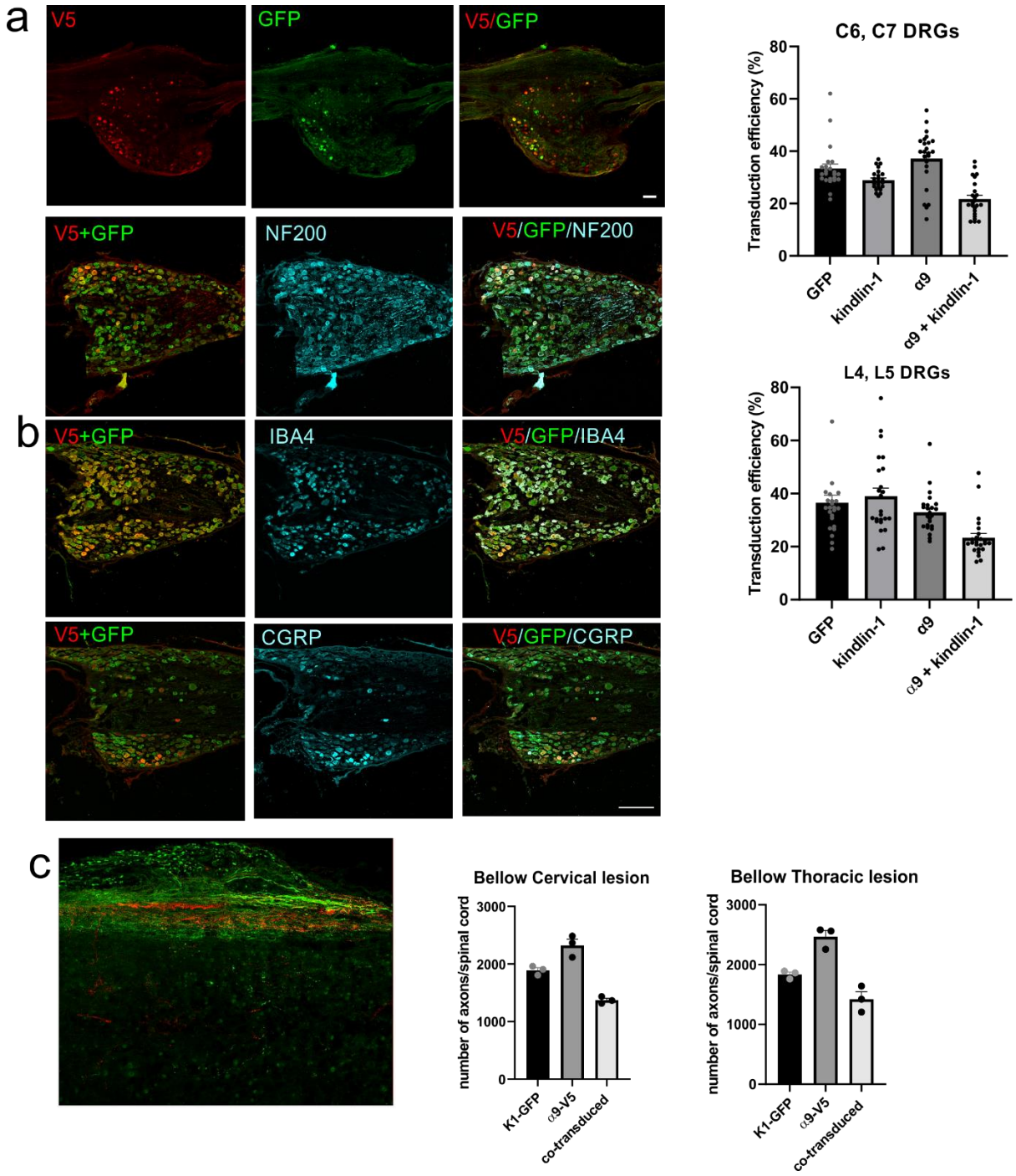

Figure 2

a) A dorsal root ganglion that was injected 13 weeks previously with AAV1-kindlin-1-GFP + AAV1- α9 – V5. Many neurons are yellow in the composite picture below, indicating co-transduction, but some neurons are red or green indicating that they were transduced by only one of the viral vectors. Bar=500um **b)** Sensory neurons of the three main types were transduced with the AAV1 vectors. CGRP, IBA4 and NF200 immunostaining (middle column) overlaps with V5 and GFP staining showing integrin and kindlin (left and right composite columns) Bar = 200µm **c)** Axons caudal to the lesion stained for V5

and GFP. Many of the axons contain both integrin and kindlin, but there are axons that are only positive for one or the other.

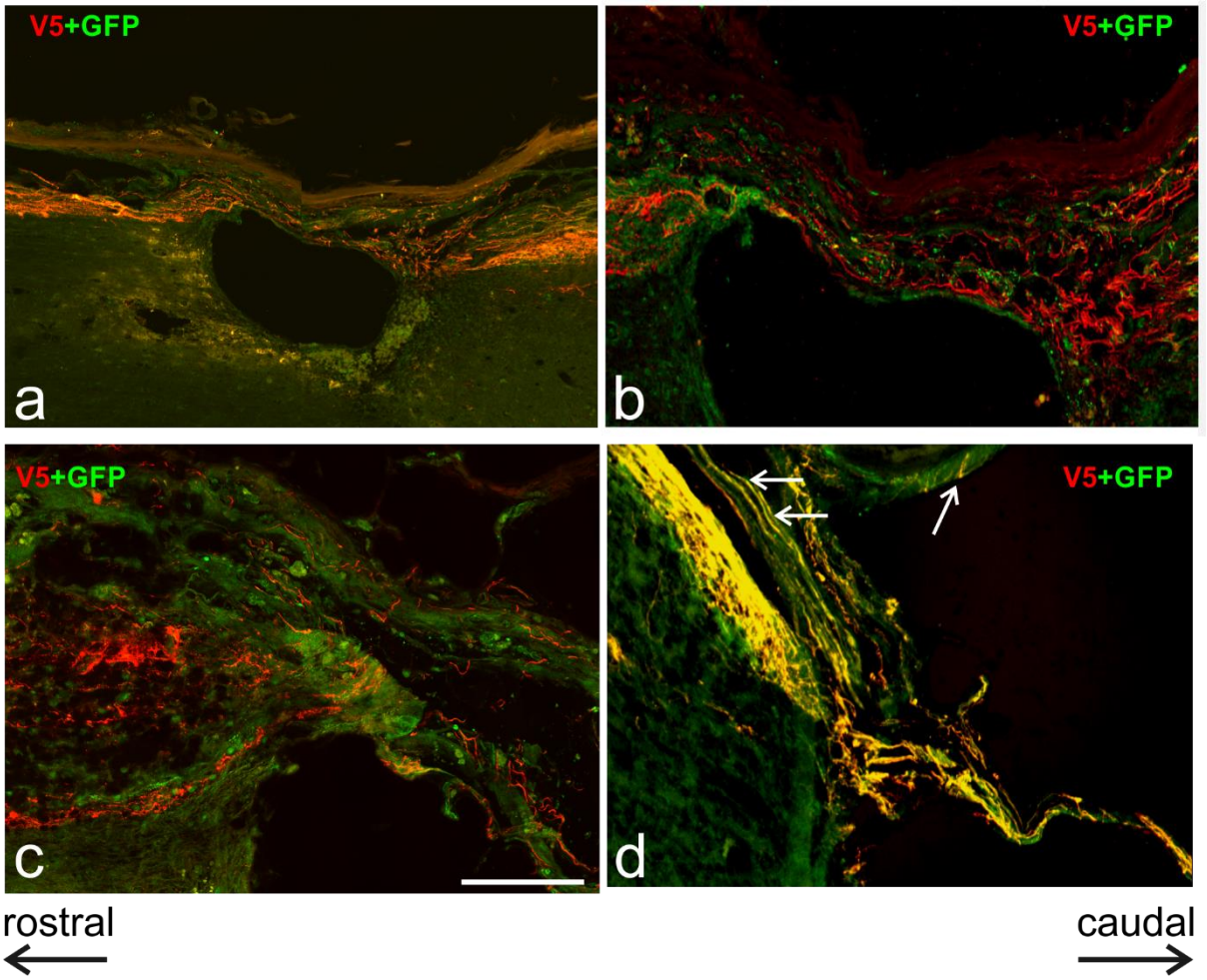

Figure 3

a,b) Two examples of spinal lesions at T10 from the α9-kindlin group. Many red (α9-V5 stained) axons approach the lesion from the right (caudal). There is some random growth as they enter the the bridge across the top of the lesion that is mostly composed of meningeal cells, then the axons re-enter CNS tissue to grow rostrally on the left. **c)** An example of axons passing through a fine connective tissue strand. At the rostral end (left) there is a region of wandering growth as the axons re-enter CNS tissue. **d)** Where axons reach the point where connective tissue strands interface with CNS tissue, some axons continue to grow in the meninges (arrows). Bars = c 1µm

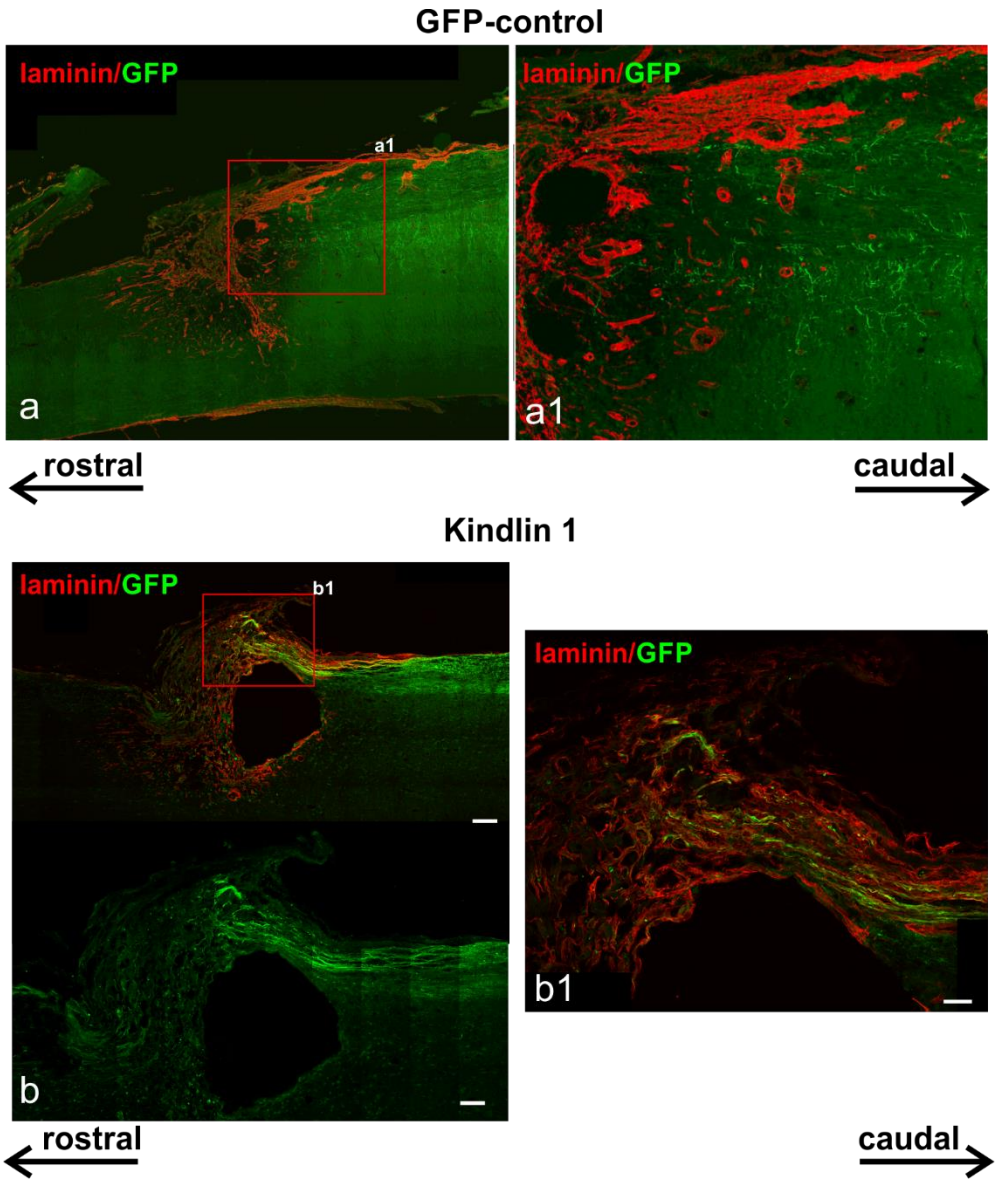

Figure 4

a) A lesion from the GFP group immunostained for GFP and laminin. GFP+ve axons are seen caudal to the lesion (right), but none have regenerated into the laminin+ve connective tissue in the lesion. **b)** Axon regeneration example from the kindlin-1 group. Axons have regenerated into the laminin+ve connective tissue in the bridge region over the lesion, and are closely associated with laminin+ve processes. No axons have grown out of the connective tissue back into CNS tissue. Bars =200 µm magnified insets 50 µm

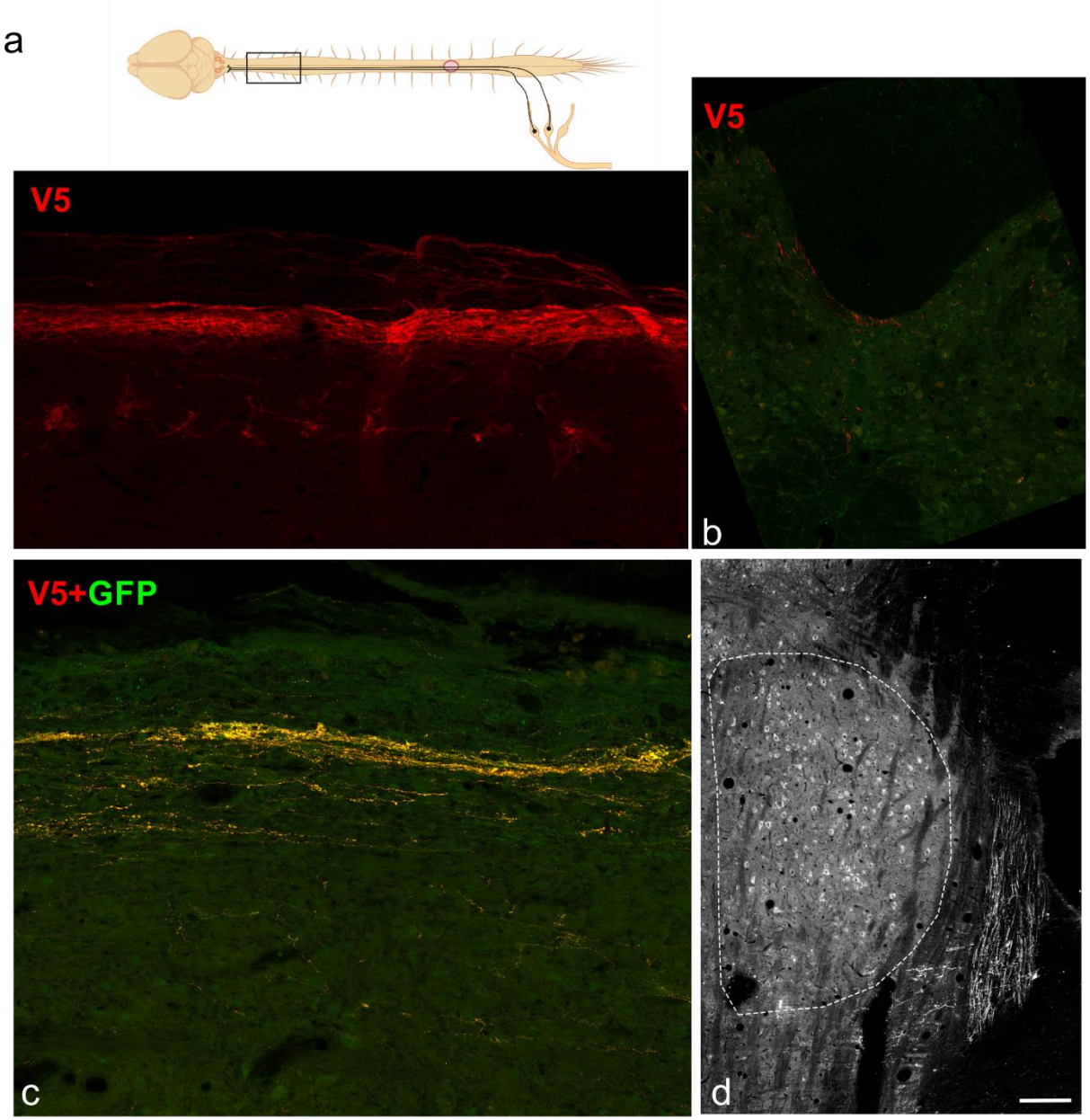

Figure 5

a) α9-V5 labelled axons in the cervical cord from an animal from the α9-kindlin group with a thoracic lesion and AAV injections to the L4,5 DRGs. Many axons are seen in a layer between dorsal horn and dorsal column white matter, and some axons are seen in the dorsal horn white matter. Rostral is to the left. **b)** Axons at level C3 labelled for α9-V5. The axons are following a pathway at the margin between the dorsal horn and the dorsal column with branches to the dorsal horn. **c)** Axons rostral to the lesion double-stained for α9-V5 and kindlin-1-GFP. All the animals are stained for both molecules. **d)** V5-stained axons in the medulla with the cuneate nucleus above. The bundle of axons approaches the edge of the nucleus and some grow towards it but not into it. There are no labelled axons in the nucleus indicating that there are no unlesioned sensory axons. Bars = 100 µm

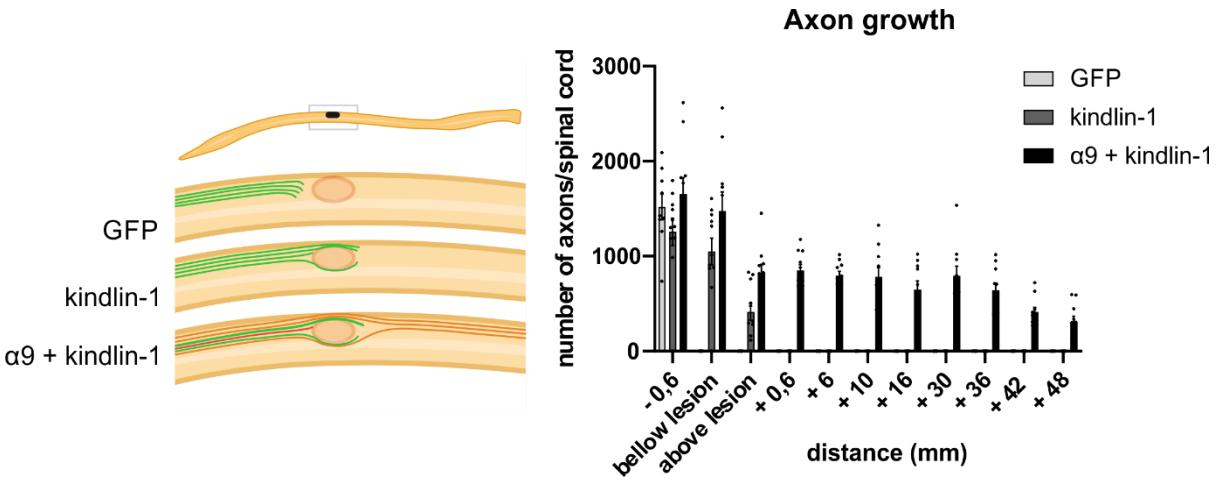

Figure 6

Diagrammatic representation of the key results of this study. Only in the α9-kindlin group was there substantial regeneration beyond the lesion into the rostral cord. In the kindlin group axons regenerated in the laminin-containing connective tissue in the lesion core. Axon counts are shown in the graph. Around 800 sensory axons grew into the rostral cord in the α9-kindlin group, numbers declining slightly as they approached the hindbrain. 5cm from the lesion is the distance to the medulla, where regenerated axons were seen. Created in Biorender

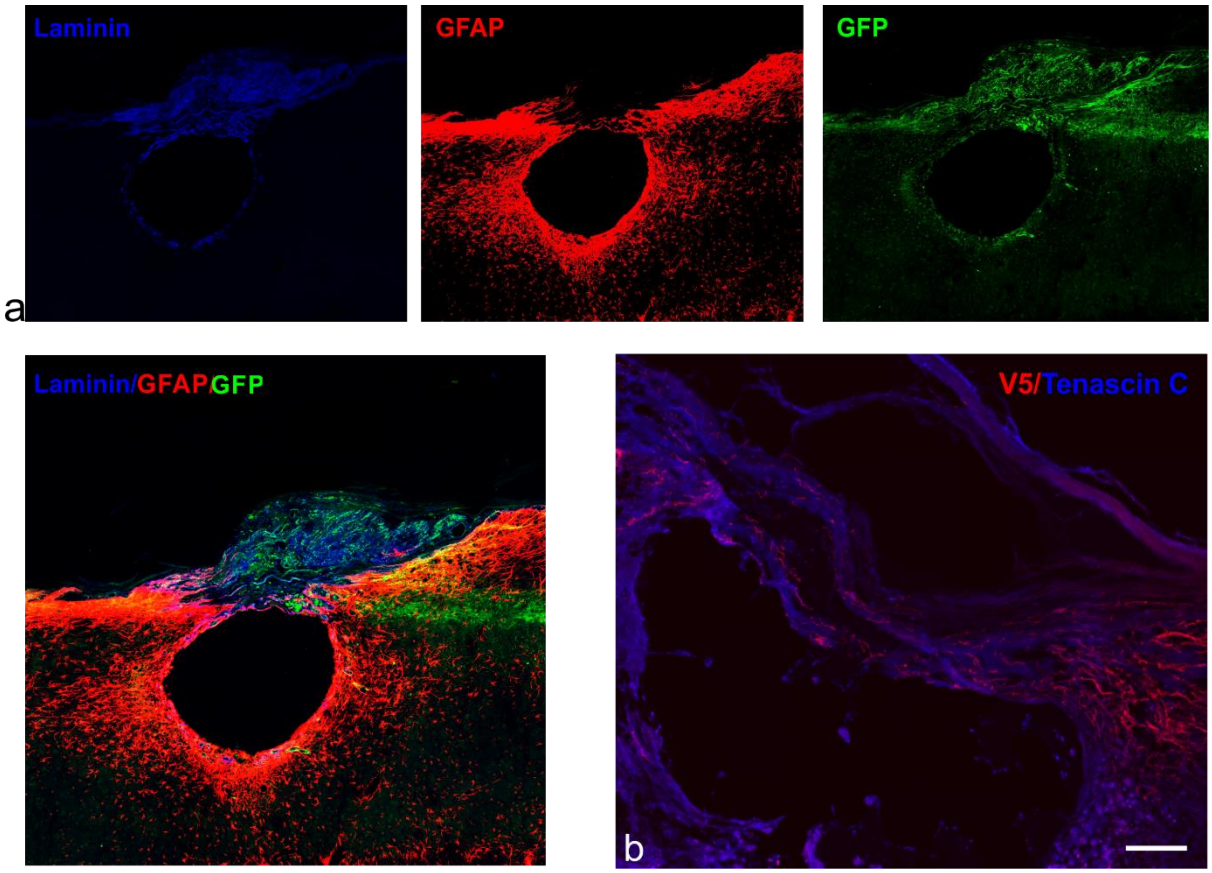

Figure 7

a) The bridge region that develops over lesions is shown. This is mostly derived from meningeal tissue and is therefore GFAP-ve, laminin+ve as in this picture. Tangled axons and axons crossing the lesion in this cord from the α9-kindlin group are seen inside the connective tissue bridge. **b)** Axon growth in the α9-kindlin group through connective tissue strands that are tenascin-C stained. Many axons with a typical regenerated morphology are seen within the strands, then entering CNS tissue rostral to the lesion on the left. Bar = 100 µm

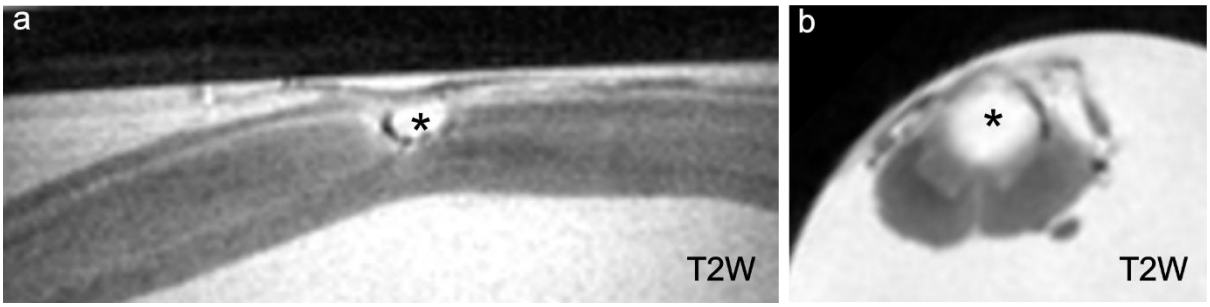

Figure 8

MRI T2 weighted pictures in longitudinal and transverse orientations to show a typical lesion. These pictures were taken from spinal cords removed from animals after fixation at week 13.

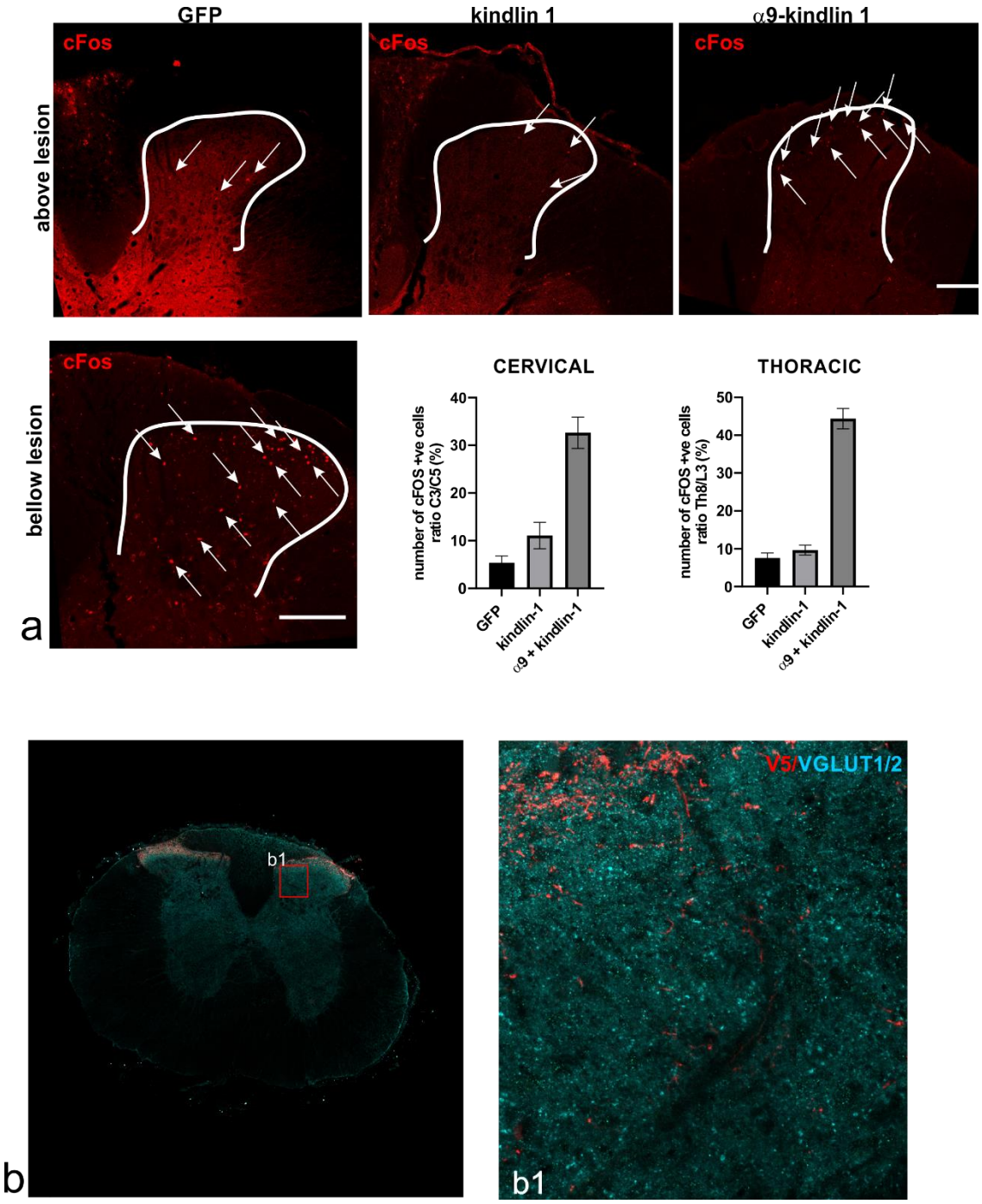

Figure 9

a) cFos stains from spinal cord dorsal horn (marked by white line) following peripheral nerve stimulation. Below the lesion many neurons (arrows) are activated by stimulation. 1cm rostral to the lesion there are few activated neurons (arrows) in the GFP and kindlin-1 groups, many more (arrows) in the α9-kindlin group indicating that functional connections were made. Number of cFos positive cells is expressed as ratio of positive cells bellow and above cervical and thoracic lesion. Scale bars = 200 µm. **b)**

High resolution images of the dorsal horn 1cm rostral to the lesion from the α9-kindlin group. Red V5-positive axons are seen growing into the grey matter with swellings on them that also stain for VGLUT2.

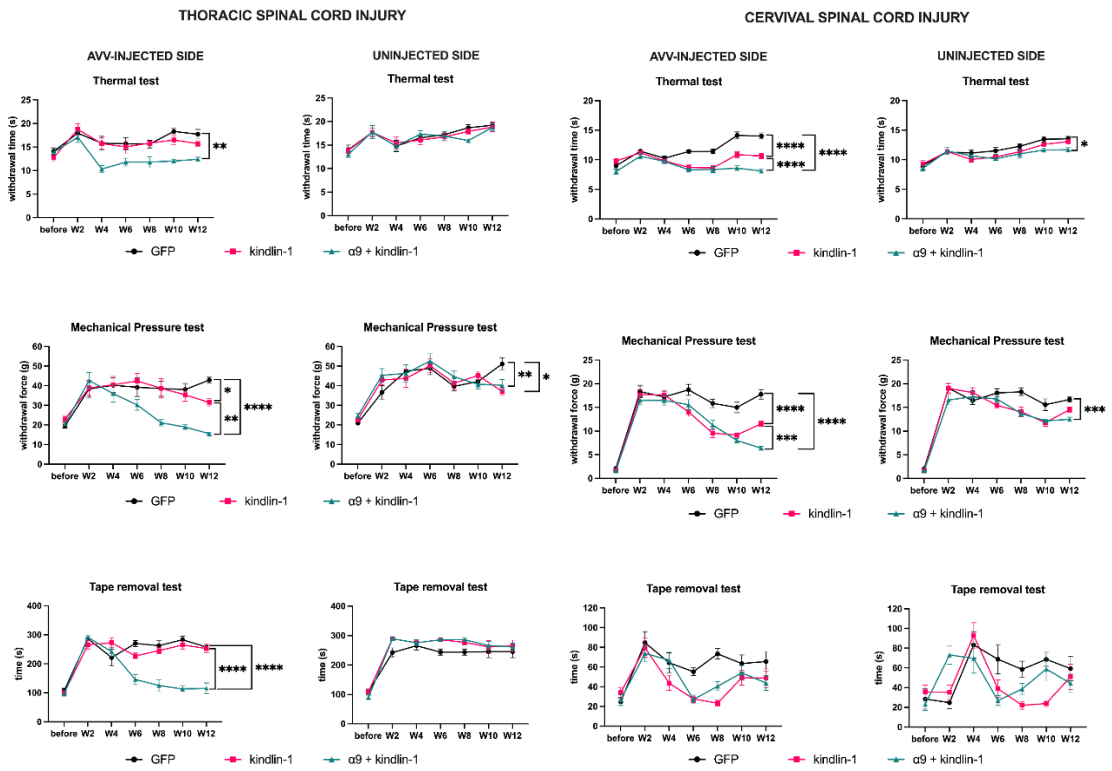

Figure 10

Sensory testing results from animals that received a T10 lesion and injection of the L4,5 DRGs (left) and that received a C4 lesion and injection of the C6,7 DRGs. After thoracic lesions, recovery in heat sensation, pressure sensation and tape removal was only seen in the α9-kindlin group and only on the treated side. In the cervical lesions there was also some recovery in the kindlin-1 group.